

11-20-1999

Subsidence, mixing, and denitrification of Arctic polar vortex air measured during POLARIS

M. Rex

Jet Propulsion Laboratory

R. J. Salawitch

Jet Propulsion Laboratory

G. C. Toon

Jet Propulsion Laboratory

B. Sen

Jet Propulsion Laboratory

J. J. Margitan

Jet Propulsion Laboratory

See next page for additional authors

Follow this and additional works at: https://scholars.fhsu.edu/chemistry_facpubs

 Part of the [Chemistry Commons](#)

Recommended Citation

Rex, M., et al. (1999), Subsidence, mixing, and denitrification of Arctic polar vortex air measured during POLARIS, *J. Geophys. Res.*, 104(D21), 26611– 26623, doi:10.1029/1999JD900463.

This Article is brought to you for free and open access by the Chemistry at FHSU Scholars Repository. It has been accepted for inclusion in Chemistry Faculty Publications by an authorized administrator of FHSU Scholars Repository.

Authors

M. Rex, R. J. Salawitch, G. C. Toon, B. Sen, J. J. Margitan, G. B. Osterman, J. F. Blavier, R. S. Gao, S. Donnelly, E. Keim, J. Neuman, D. W. Fahey, C. R. Webster, D. C. Scott, R. L. Herman, R. D. May, E. J. Moyer, M. R. Gunson, F. W. Irion, A. Y. Chang, C. P. Rinsland, and T. P. Bui

Subsidence, mixing, and denitrification of Arctic polar vortex air measured During POLARIS

M. Rex¹, R. J. Salawitch¹, G. C. Toon¹, B. Sen¹, J. J. Margitan¹, G. B. Osterman¹, J.-F. Blavier¹, R. S. Gao¹, S. Donnelly², E. Keim², J. Neuman², D. W. Fahey², C. R. Webster¹, D. C. Scott¹, R. L. Herman¹, R. D. May¹, E. J. Moyer¹, M. R. Gunson¹, F. W. Irion¹, A. Y. Chang¹, C. P. Rinsland³, and T. P. Bui⁴

Abstract. We determine the degree of denitrification that occurred during the 1996–1997 Arctic winter using a technique that is based on balloon and aircraft borne measurements of NO_y , N_2O , and CH_4 . The $\text{NO}_y/\text{N}_2\text{O}$ relation can undergo significant change due to isentropic mixing of subsided vortex air masses with extravortex air due to the high nonlinearity of the relation. These transport related reductions in NO_y can be difficult to distinguish from the effects of denitrification caused by sedimentation of condensed HNO_3 . In this study, high-altitude balloon measurements are used to define the properties of air masses that later descend in the polar vortex to altitudes sampled by the ER-2 aircraft (i.e., ~20 km) and mix isentropically with extravortex air. Observed correlations of CH_4 and N_2O are used to quantify the degree of subsidence and mixing for individual air masses. On the basis of these results the expected mixing ratio of NO_y resulting from subsidence and mixing, defined here as NO_y^{**} , is calculated and compared with the measured mixing ratio of NO_y . Values of NO_y and NO_y^{**} agree well during most parts of the flights. A slight deficit of NO_y versus NO_y^{**} is found only for a limited region during the ER-2 flight on April 26, 1997. This deficit is interpreted as indication for weak denitrification (~2–3 ppbv) in that air mass. The small degree of denitrification is consistent with the general synoptic-scale temperature history of the sampled air masses, which did not encounter temperatures below the frostpoint and had relatively brief encounters with temperatures below the nitric acid trihydrate equilibrium temperature. Much larger degrees of denitrification would have been inferred if mixing effects had been ignored, which is the traditional approach to diagnose denitrification. Our analysis emphasizes the importance of using other correlations of conserved species to be able to accurately interpret changes in the $\text{NO}_y/\text{N}_2\text{O}$ relation with respect to denitrification.

1. Introduction

Rapid loss of ozone in the Arctic vortex during winter and spring is caused by catalytic cycles driven by active chlorine species ($\text{ClO}_x = \text{Cl}, \text{ClO}, \text{Cl}_2\text{O}_2$) [e.g., Salawitch *et al.*, 1990; Waters *et al.*, 1993]. Elevated levels of ClO_x result from heterogeneous reactions of HCl and ClONO_2 on polar stratospheric cloud (PSC) particles, which form at low temperatures during winter in the Arctic region [e.g., Brune *et al.*, 1990; Webster *et al.*, 1993; Notholt *et al.*, 1995]. Following the evaporation of PSCs, the lifetime of elevated ClO_x , and hence the time period of rapid ozone loss, is mainly controlled by the amount of NO_2 in the vortex [e.g., Brune *et al.*, 1991; Salawitch *et al.*, 1993]. Levels of NO_2 are quite small during the Arctic winter due to heterogeneous conversion of NO_x (NO, NO_2) to HNO_3 [e.g., Kawa *et al.*, 1992]. In spring, the production rate of NO_2 from the photolysis of HNO_3 rises due to the increase in the intensity of solar UV irradiance in the lower stratosphere.

The released NO_2 reacts rapidly with ClO to form the passive reservoir species ClONO_2 [e.g., Toon *et al.*, 1992; Roche *et al.*, 1994]. This mechanism effectively slows down the Arctic ozone loss rate in spring and limits the overall loss of ozone in the Arctic vortex [e.g., Brune *et al.*, 1991; Salawitch *et al.*, 1993].

Denitrification, the permanent removal of NO_y (total reactive nitrogen) by the sedimentation of HNO_3 -bearing PSC particles, leads to reduced production of NO_2 during spring [Toon *et al.*, 1986]. Widespread severe denitrification is common in the Antarctic [e.g., Toon *et al.*, 1989; Fahey *et al.*, 1990; Santee *et al.*, 1995] because of the extremely low wintertime temperatures. In the warmer Arctic, patches of denitrified air have also been observed after exceptionally cold winters [e.g., Fahey *et al.*, 1990; Huebler *et al.*, 1990; Oelhaf *et al.*, 1996; Arnold *et al.*, 1998; Hints *et al.*, 1998]. For the Arctic winter of 1995–1996, the coldest on record, the period of ozone destruction was so prolonged by denitrification that the overall ozone loss reached record values in the layer of air that experienced the longest period of cold conditions (favorable for denitrification) [Rex *et al.*, 1997]. Recent model calculations have shown that higher degrees of Arctic denitrification in the future, related perhaps to stratospheric cooling due to the build-up of greenhouse gases, would lead to larger seasonal ozone depletion despite the projected decline in inorganic chlorine [Waibel *et al.*, 1999].

The degree of denitrification in a given air mass has been typically estimated by comparison of measured mixing ratios of NO_y with the expected abundance of NO_y (defined as NO_y^*) calculated

¹Jet Propulsion Laboratory, California Institute of Technology, Pasadena, California.

²Aeronomy Laboratory, NOAA, Boulder, Colorado.

³NASA Langley Research Center, Hampton, Virginia.

⁴NASA Ames Research Center, Moffett Field, California.

from simultaneous observations of N_2O and well-established correlations between the mixing ratios of NO_x and N_2O [e.g., *Toon et al.*, 1989; *Fahey et al.*, 1990; *Rinsland et al.*, 1999]. This method is based on the assumption that the mixing ratios of two long-lived tracers (i.e., chemical lifetime long compared to mixing lifetime) develop a compact relationship independent of altitude and latitude [*Plumb and Ko*, 1992]. Severe denitrification is common throughout the Antarctic vortex and can be inferred in a straightforward manner by examination of the NO_x versus N_2O relation [e.g., *Fahey et al.*, 1990]. This method can also be used in the Arctic provided that mixing does not change the tracer relations prior to denitrification. For instance, the observation of a patchy structure of severe NO_x deficits and the nearby presence of air masses with the established $\text{NO}_x/\text{N}_2\text{O}$ correlation indicates that mixing did not change the $\text{NO}_x/\text{N}_2\text{O}$ relation prior to the onset of denitrification for the winter of 1988–1989 [*Fahey et al.*, 1990].

In contrast to the picture of well-preserved tracer/tracer relationships that can be changed only by chemistry or denitrification, *Waugh et al.* [1997], *Michelsen et al.* [1998] and *Kondo et al.* [1999] have recently shown that mixing of subsided innervortex with extravortex air masses can lead to substantial changes in the $\text{NO}_x/\text{N}_2\text{O}$ relationship without denitrification. *Michelsen et al.* [1998] and *Kondo et al.* [1999] have also suggested that dynamically induced changes in the $\text{NO}_x/\text{N}_2\text{O}$ correlation can be mistaken for denitrification. The NO_x versus N_2O relation is highly nonlinear, making it particularly sensitive to changes induced by descent and mixing [*Waugh et al.*, 1997; *Michelsen et al.*, 1998; *Kondo et al.*, 1999] (discussed in more detail in section 3.1.). *Waugh et al.* [1997] has noted more generally that the unique tracer/tracer relationships in the *Plumb and Ko* [1992] framework are not preserved under the special conditions of the polar vortices where redistribution of tracers by vertical transport is comparably fast to isentropic (quasi-horizontal) mixing. *Waugh et al.* [1997] showed examples of a change in the relationship of several pairs of long-lived tracers that was connected with mixing processes in the vicinity of the polar vortex. In the Arctic vortex, severe denitrification is rare [e.g., *Santee et al.*, 1995; *Rinsland et al.*, 1999], and changes in the $\text{NO}_x/\text{N}_2\text{O}$ relationship caused by descent and isentropic mixing can easily mask changes caused by moderate denitrification.

The focus of this paper is to account for changes in the $\text{NO}_x/\text{N}_2\text{O}$ relationship due to descent and isentropic mixing so that the degree of denitrification can be accurately quantified. The tracer/tracer relationship of a pair of long-lived tracers that does not include NO_x is first examined to quantify the dynamically induced changes that affect the measured airmasses. The selected pair of tracers should have a long chemical lifetime in the stratosphere. Dynamically induced changes can only be quantified if the tracer/tracer relationship prior to isentropic mixing are nonlinear. *Michelsen et al.* [1998] and *Kondo et al.* [1999] have shown that the $\text{CH}_4/\text{N}_2\text{O}$ relationship can be used to assess the influence of descent and mixing because the extravortex correlation of these gases exhibits significant curvature [*Herman et al.*, 1998; *Michelsen et al.*, 1998] and because both gases are long-lived (the lifetime of CH_4 is longer than 1 year below 40 km and ~ 250 days at 50 km, the lifetime of N_2O is longer than 1 year below 35 km, ~ 200 days at 40 km and ~ 2 months at 50–55 km; the lifetimes have been estimated for 60°N during mid-October, using the model described by *Osterman et al.* [1997]). During the Photochemistry of Ozone Loss in the Arctic Region in Summer (POLARIS) campaign measurements of CH_4 and N_2O gases have been obtained by instruments onboard the ER-2 as well as by the balloon-borne MkIV and ALIAS II instruments at high latitude.

As will be shown in sections 3.2. and 3.7., the in situ observations obtained during POLARIS clearly show distinct “mixing

lines” in the $\text{CH}_4/\text{N}_2\text{O}$ relationship on individual isentropic surfaces. A mixing line refers to the tracer/tracer correlation pattern that results from various mixtures of two air masses, at the same potential temperature level, with distinctly different composition resulting from their dynamical histories (e.g. a midlatitude air parcel with high values of N_2O and CH_4 and a vortex air parcel with low values of N_2O and CH_4). Our approach for estimating denitrification differs somewhat from the method used by *Michelsen et al.* [1998] in which mixing lines in tracer/tracer plots were assembled over a wide range of potential temperatures from points along a vertical profile. The end points of these lines cannot be interpreted as end-members of isentropic mixing processes because they have not been at similar potential temperatures at any time during the winter. Recently, R. A. Plumb et al. (The effects of mixing on tracer relationships in the polar vortices, submitted to *Journal of Geophysical Research*, 1999) (hereinafter referred to as Plumb et al., submitted manuscript, 1999) have shown that relatively straight lines can evolve in profile measurements of tracer/tracer relationships that cover a wide range of potential temperatures if there is continuous mixing into the polar vortex concurrent with descent inside the vortex. Quantification of the influence of mixing under these circumstances remains difficult. In this paper, however, we show how changes in the $\text{NO}_x/\text{N}_2\text{O}$ relationship due to mixing can be accurately quantified, given that isentropic mixing lines (rather than lines covering a wide range of potential temperatures) can be identified from the $\text{CH}_4/\text{N}_2\text{O}$ relation. Our quantitative results are contingent on the assumption that the change in the tracer/tracer relations due to mixing took place following the bulk of the descent inside the polar vortex. The validity of this assumption is discussed in sections 3.4 and 4.

2. Data Sets

In this work, we utilize observations obtained by instruments aboard the NASA ER-2 aircraft and several balloon borne instruments during the POLARIS mission. Instruments aboard the ER-2 provided in situ measurements of many important stratospheric gases for a wide range of latitudes and altitudes near 20 km. During POLARIS, balloon-borne observations complemented the ER-2 measurements by providing vertical profiles of stratospheric gas concentrations using both in situ and remote sensing techniques.

Measurements aboard the ER-2 of N_2O and CH_4 were made by the Aircraft Laser Infrared Absorption Spectrometer (ALIAS). ALIAS is a scanning tunable diode laser spectrometer that measures CH_4 , N_2O , HCl, and CO using high-resolution laser absorption in the 3–8 μm wavelength region [*Webster et al.*, 1994]. ALIAS II provided in situ measurements of CH_4 and N_2O from the Observations from the Middle Stratosphere (OMS) in situ balloon gondola. ALIAS and ALIAS II measure N_2O and CH_4 with an estimated 5% accuracy and precisions of 1% and 5%, respectively [*Herman et al.*, 1998]. ER-2 measurements of NO_x were made by the National Oceanic and Atmospheric Administration (NOAA) Aeronomy Laboratory reactive nitrogen instrument. The instrument measures total nitrogen by catalytically reducing NO_x to NO then detecting NO through chemiluminescent reaction with O_3 . NO_x is measured with a total 1 σ uncertainty of <15% [*Fahey et al.*, 1989]. Here we examine ER-2 observations obtained on the two poleward flights from Fairbanks, Alaska (65°N, 148°W), that encountered polar vortex air (April 26 and June 30, 1997) and the OMS observations obtained on June 30, 1997, from a balloon flight over Fairbanks.

The MkIV Fourier Transform Infra-Red (FTIR) spectrometer [*Toon*, 1991] obtains remote measurements of the composition of the atmosphere using the solar occultation technique. The bright-

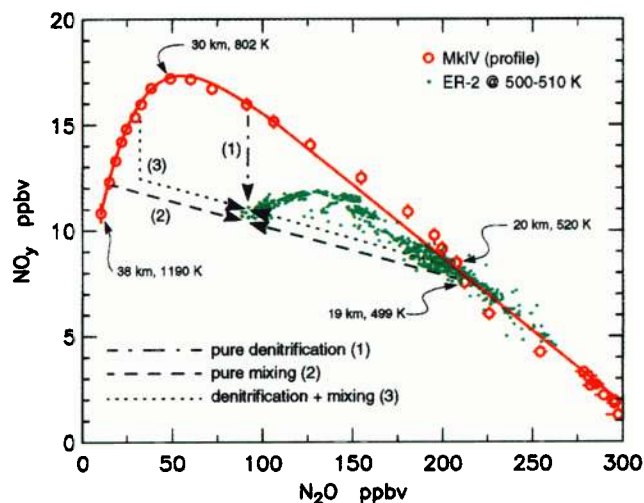


Plate 1. $\text{NO}_y/\text{N}_2\text{O}$ correlations measured during the MkIV flight on May 8, 1997 and during the ER-2 flight on April 26, 1997. The MkIV data represent a vertical profile between 8 and 38 km altitude. The potential temperatures of some data points are indicated in the plot. The spacing between points is 1 km. The error bars denote the 1σ precision of the MkIV measurements. The red line is a composed polynomial fit to the MkIV data (4th-order fit for N_2O volume mixing ratios (vmrs) < 125 ppbv, linear fit for N_2O vmrs > 125 ppbv). All ER-2 data points have been measured between potential temperatures of 500 and 510 K. The ER-2 NO_y measurements were obtained by the NOAA chemiluminescent instrument with a 1σ total uncertainty of better than 10%; the ER-2 N_2O measurements were made by the ALIAS diode laser instrument with a 1σ total uncertainty of 5% (1% precision). The dashed, dotted, and dash-dotted lines illustrate scenarios with different degrees of denitrification and descent that could explain the low mixing ratios of NO_y observed by the ER-2 at mixing ratios of N_2O below 100 ppbv.

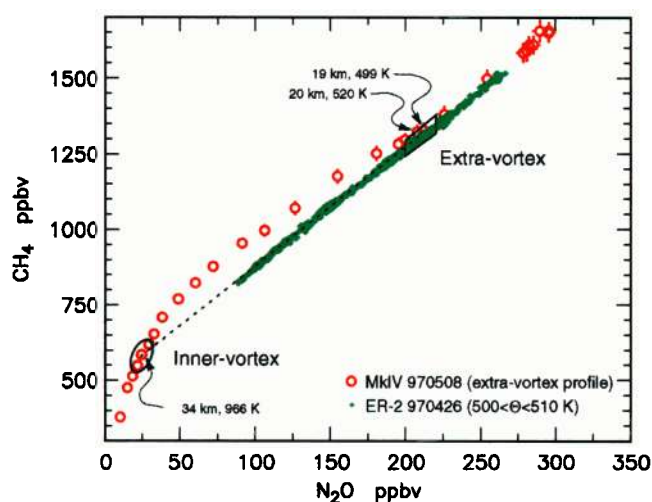


Plate 3. $\text{CH}_4/\text{N}_2\text{O}$ correlation measured by the MkIV on May 8, 1997, and the ER-2 ALIAS instrument on the same flight as in Plate 1. The 1σ total uncertainty of both the ALIAS CH_4 and N_2O measurements is 5% (1% precision). The error bars for the MkIV measurement denote the 1σ precision. The mixing line for the ER-2 measurements is indicated by the dotted line. The regions where the mixing line intersects the extravortex reference correlation denote the air masses that have mixed to produce the properties observed by the ER-2 along the mixing line. The innervortex and extravortex mixing end-members are indicated. The altitudes and potential temperatures of the MkIV measurements in these regions are shown.

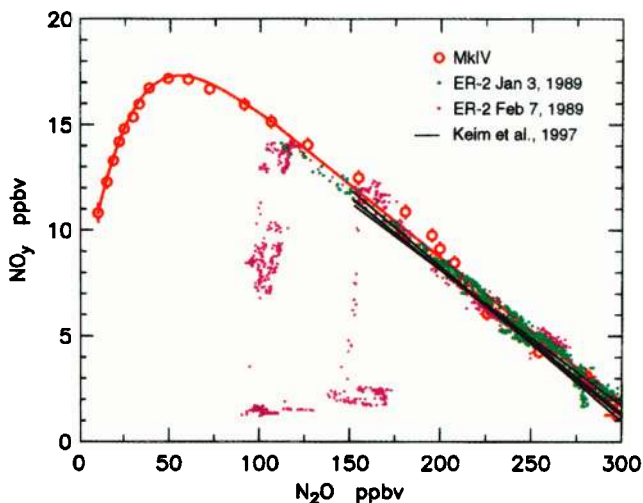


Plate 2. As in Plate 1, but for ER-2 data measured during an early winter and a mid-winter flight during the Airborne Arctic Stratospheric Experiment (AASE) in 1989. The ER-2 data has not been filtered by Θ . The ER-2 observations of N_2O were obtained by the ATLAS instrument with a 1σ total uncertainty of 3%. They were obtained for temperatures above T_{NAT} (see text for an explanation of T_{NAT}). However, the average temperature near 20 km during January 1989 was lower than observed during the 26 years prior to 1989 and the minimum temperature in the vortex was persistently below T_{NAT} and reached the frostpoint during late January 1989. Fits to ER-2 observations in northern midlatitudes in various years and seasons [Keim et al., 1997] are also shown (black lines). The ER-2 data was normalized to 1997, assuming an increasing trend in the N_2O and NO_y mixing ratios of 0.2% per year.

ness and stability of the Sun allow high signal-to-noise ratio spectra with broad coverage ($650\text{--}5650\text{ cm}^{-1}$) to be obtained at high-spectral resolution (0.01 cm^{-1}), allowing the abundances of a large number of gases to be measured simultaneously. The retrieval algorithm, spectroscopic parameters, and measurement uncertainties are discussed by Sen et al. [1996, 1998]. Gases measured by MkIV relevant to this work include O_3 , N_2O and CH_4 . The MkIV instrument also provides a complete determination of NO_y by measuring NO , NO_2 , HNO_3 , HNO_4 , N_2O_5 and ClONO_2 individually. The measurement of CH_4 and N_2O have an accuracy and precision of 5%. The precision of NO_y for 20 km is $\sim 5\%$ with an accuracy of 15%, values which are confirmed by the comparisons between MkIV balloon and ER-2 measurements [Toon et al., this issue]. Here we examine profiles obtained by the MkIV instrument on the May 8, 1997, balloon flight near Fairbanks.

3. Data Analysis and Results

3.1. $\text{NO}_y/\text{N}_2\text{O}$ Relationship

Plate 1 shows the $\text{NO}_y/\text{N}_2\text{O}$ relationship measured at high altitude during POLARIS by the MkIV infrared spectrometer between 8 and 38 km at a vertical resolution of ~ 2 km on May 8, 1997 and by the NO_y and ALIAS instruments on board the ER-2 on an isentropic level (500–510 K) near 20 km on April 26, 1997. Potential vorticity analyses and the relation between N_2O and potential temperature (e.g. $\text{N}_2\text{O}=200$ ppbv at 500 K: typical values of N_2O inside the vortex at 500 K are much lower) indicate that the MkIV profile was obtained outside of the polar vortex.

In Plate 2 we compare the MkIV measurements to other (non-POLARIS) ER-2 $\text{NO}_y/\text{N}_2\text{O}$ measurements [Loewenstein et al., 1993] to demonstrate that the differences shown in Plate 1 are

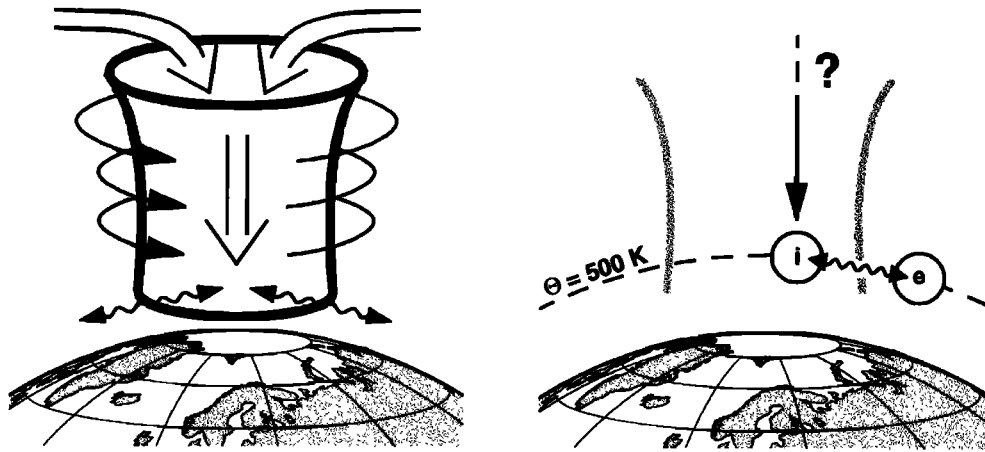


Figure 1. Illustration of the large scale descent in the polar vortex, which brings air masses from high altitudes to low potential temperature levels where they can mix with extravortex air mainly during the late vortex and vortex break up period. The descended innervortex mixing member is marked by an “i” and the extravortex mixing member is marked by an “e”. To predict the properties of the mixed air masses, the original level of the air mass “i” has to be estimated.

not platform or instrument related. The MkIV measurements of NO_y and N_2O are similar to the well established reference relationship between these tracers at mid-latitudes [e.g., *Chang et al.*, 1996; *Sen et al.*, 1998; *Keim et al.*, 1997 (black lines in Plate 2)] and agree well with earlier measurements obtained by ER-2 instruments at similar latitudes during the Arctic winter (e.g. the flight on January 3, 1989, green points in Plate 2). For mixing ratios of N_2O below ~ 100 ppbv, the relation between $\text{NO}_y/\text{N}_2\text{O}$ is highly nonlinear and exhibits a peak near 30 km due to rapid loss of NO_y at high altitudes due to the reaction $\text{N} + \text{NO}$ [e.g., *Russell et al.*, 1988; *Nevison and Holland*, 1997]. The $\text{NO}_y/\text{N}_2\text{O}$ relationship measured by MkIV (Plate 1) is used in this work to represent the conditions in the vortex prior to denitrification, descent, and isentropic mixing. Compared with this reference relation, severe NO_y deficits were observed in the Arctic during a number of ER-2 flights in February 1989 (e.g. the flights on February 7, 1989, magenta points in Plate 2). In contrast, the ER-2 observations obtained inside the Arctic vortex on April 26, 1997 during POLARIS show only moderate deficits of NO_y compared to the reference $\text{NO}_y/\text{N}_2\text{O}$ relationship for air with mixing ratios of N_2O below ~ 200 ppbv (Plate 1).

The moderate deficit of NO_y observed during POLARIS could be due to one of several processes: (1) denitrification, (2) descent followed by isentropic mixing, and (3) a combination of 1 and 2. Denitrification (process 1) is illustrated by the dot-dashed arrow in Plate 1: Starting from the MkIV $\text{NO}_y/\text{N}_2\text{O}$ reference correlation, this process could have reduced the NO_y mixing ratio without changing the N_2O mixing ratio. The process of descent followed by isentropic mixing (process 2) is illustrated schematically in Figure 1. During winter large scale subsidence takes place inside the vortex, which is relatively well isolated from extravortex air [e.g., *Abrams et al.*, 1996]. As the vortex weakens and finally breaks up during spring, vortex air masses irreversibly mix with air outside the vortex along surfaces of constant potential temperature [e.g., *Waugh et al.*, 1997]. The effect of process 2 on the $\text{NO}_y/\text{N}_2\text{O}$ correlation is illustrated by the dashed arrow in Plate 1. Mixing of two air masses at the same potential temperature in varying degrees (one air mass from inside the vortex, the other from outside) would lead to a linear relationship between NO_y and N_2O . If the reference tracer/tracer relation is nonlinear, the mixing between these air masses can produce a new tracer/tracer relation quite different than

the reference relation [*Waugh et al.*, 1997; *Herman et al.*, 1998; *Michelsen et al.*, 1998; *Kondo et al.*, 1999]. The combination of denitrification and mixing (process 3) is illustrated by the dotted arrow in Plate 1. In this scenario, denitrification first reduces the NO_y mixing ratio at constant N_2O (illustrated by the part of the dotted arrow that is parallel to the NO_y axis). Subsequent mixing with extravortex air (illustrated by the rest of the dotted arrow) then would produce the observed air mass properties. Recently, *Plumb et al.* (submitted manuscript, 1999) have shown that continuous isentropic mixing during descent could lead to the development of anomalous tracer/tracer relationships inside the vortex. This possibility is also discussed.

3.2. $\text{CH}_4/\text{N}_2\text{O}$ Relationship

Michelsen et al. [1998] and *Herman et al.* [1998] showed that mixing of subsided innervortex air with extravortex air tends to reduce the curvature of the $\text{CH}_4/\text{N}_2\text{O}$ relation. We use straight isentropic mixing lines in the $\text{CH}_4/\text{N}_2\text{O}$ relation at specific potential temperature levels to quantify the amount of descent that has occurred inside the vortex and the degree of mixing between vortex and extravortex air for the regions sampled by the ER-2. MkIV measurements of the $\text{CH}_4/\text{N}_2\text{O}$ correlation (red circles in Plate 3) obtained near 65°N on May 8, 1997, for extravortex air are used as the extravortex reference correlation. The MkIV $\text{CH}_4/\text{N}_2\text{O}$ correlation agrees well with that measured by ATMOS in November 1994 between 40° and 50°N [*Chang et al.*, 1996]. A pronounced curvature is visible in the extravortex $\text{CH}_4/\text{N}_2\text{O}$ correlation for mixing ratios of N_2O below 250 ppbv. In contrast, observations obtained on April 26, 1997 near 20 km by the ER-2 ALIAS instrument reveal a nearly linear correlation between CH_4 and N_2O (green dots in Plate 3) that deviates significantly from the extravortex correlation. The low mixing ratios of N_2O between 500 and 510 K potential temperature indicate that subsided polar vortex air masses were sampled by the ER-2 during this flight.

Since the correlation between the mixing ratios of these long-lived tracers cannot be changed by reversible transport or chemistry, the most obvious explanation for the ER-2 observations is mixing of extravortex air with polar vortex air that has subsided from higher altitudes [e.g., *Waugh et al.*, 1997]. The two air masses

that must have mixed isentropically to produce the observed $\text{CH}_4/\text{N}_2\text{O}$ relations along the linear mixing line are referred to as the “innervortex end-member” and the “extravortex end-member”. It is reasonable to assume that the bulk of the mixing took place in spring, following the strongest descent within the vortex (this assumption is discussed in section 4). Therefore the composition of the extravortex end-member (the trapezoid marked in Plate 3) is defined by the ambient mixing ratios of CH_4 and N_2O observed outside of the vortex by the ER-2 and by the MkIV instrument at the same potential temperature level of the ER-2 flight. The composition of the innervortex end-member is defined by the intersection of the extrapolated ER-2 mixing line and the MkIV reference correlation (oval region in Plate 3). Since the $\text{CH}_4/\text{N}_2\text{O}$ relation is nearly linear between 15 and 40 ppbv N_2O , inhomogeneous descent inside the polar vortex (provided that the air masses originate from this near-linear region) followed by isentropic mixing of these vortex air masses with each other would not change the $\text{CH}_4/\text{N}_2\text{O}$ relationship in the innervortex end-member considerably. The fractional contribution of the innervortex and the extravortex end-members to specific ER-2 observations along the $\text{CH}_4/\text{N}_2\text{O}$ mixing line is determined from the relative distance of the observed N_2O mixing ratio to that of both end-members.

3.3. Calculation of NO_y^{**}

We use the notation NO_y^{**} to refer to the mixing ratio of NO_y that would have been present in the absence of denitrification, after accounting for the effects of descent and isentropic mixing. For the limit of unmixed air masses this quantity is identical to NO_y^* [Fahney et al., 1989] which is based only on the reference correlation and does not account for descent and mixing. The value of NO_y^{**} is calculated on a point-by-point basis along the flight track of the ER-2 by considering isentropic mixing between the innervortex and extravortex end-members derived from our analysis of simultaneous measurements of CH_4 and N_2O . As described in section 3.2, the mixing ratio of N_2O associated with the innervortex end-member (here defined as $[\text{N}_2\text{O}]_i$) was calculated based on the intersection with the reference relation of a straight line passing through two points: one defined by the measured mixing ratios of CH_4 and N_2O and the other defined by the extravortex end-member. The composition of the extravortex end-member used for all ER-2 observations considered here, which were obtained for potential temperatures between 500 and 530 K, is defined by the trapezoid in Plate 3. The NO_y mixing ratios of both end-members can be estimated from the respective mixing ratios of N_2O and the $\text{NO}_y/\text{N}_2\text{O}$ correlation measured by the MkIV instrument on May 8, 1997. Values of NO_y^{**} have been calculated from the NO_y mixing ratios of both end-members and their fractional contribution to the mixed air mass:

$$\text{NO}_y^{**} = \frac{[\text{N}_2\text{O}] - [\text{N}_2\text{O}]_i}{[\text{N}_2\text{O}]_e - [\text{N}_2\text{O}]_i} [\text{NO}_y]_e + \left(1 - \frac{[\text{N}_2\text{O}] - [\text{N}_2\text{O}]_i}{[\text{N}_2\text{O}]_e - [\text{N}_2\text{O}]_i} \right) [\text{NO}_y]_i \quad (1)$$

where $[\text{N}_2\text{O}]$ denotes the mixing ratio of N_2O of the respective air mass and the variables with indices e and i denote the properties of the extravortex and innervortex mixing end-members, respectively. The uncertainties of the calculated parameters including NO_y^{**} have been estimated based on the uncertainty of the composition of the extravortex end-member (indicated by the size of the trapezoid in Plate 3) and the precisions of the measurements.

3.4. Underlying Assumptions

Two critical assumptions for our analysis are (1) the ability to directly combine remote (MkIV) and in situ (ER-2 and OMS) observations of NO_y , CH_4 , and N_2O acquired by vastly different techniques without corrections for possible systematic differences and (2) the validity of using the $\text{NO}_y/\text{N}_2\text{O}$ and $\text{CH}_4/\text{N}_2\text{O}$ reference relations that have been measured outside the polar vortex to represent the innervortex end-member for the mixing processes analyzed here. Assumption (1) is supported by the remarkably good agreement between the MkIV reference correlation for $\text{NO}_y/\text{N}_2\text{O}$ and the ER-2 observations obtained in the Arctic vortex during January and February 1989 (Plate 2). Comparisons of MkIV and ER-2 observations of NO_y and N_2O obtained at mid-latitudes [Sen et al., 1998, Figure 2] and of ATMOS and ER-2 observations of NO_y , CH_4 , and N_2O ([Chang et al., 1996, Figure 3] ATMOS acquires observations using solar occultation in a manner similar to the MkIV instrument) lend further confidence in the agreement of the different sources of data. Toon et al. [1999] conclude that the bias between the MkIV and ALIAS measurements of N_2O is only 2%. Finally, the excellent agreement between the MkIV $\text{CH}_4/\text{N}_2\text{O}$ reference relation and ALIAS II observations obtained at high latitude during POLARIS for extravortex air (discussed in section 3.7) provides additional support for the validity of assumption (1). Furthermore, the $\text{NO}_y/\text{N}_2\text{O}$ and $\text{CH}_4/\text{N}_2\text{O}$ relations measured at northern mid-latitudes during November 1994 by ATMOS [Chang et al., 1996] agree well with the MkIV reference relations used here (the agreement between MkIV and ATMOS measurements of CH_4 and N_2O is discussed further in section 3.7).

Assumption (2) cannot be fully tested for the winter of 1996-1997 since tracer measurements inside the Arctic vortex are not available during the different phases of the winter. Measurements of CH_4 and N_2O obtained during February 1997 from two balloon flights over Kiruna, Sweden (68°N) [Kondo et al., 1999] represent conditions near the vortex edge and therefore can not properly be interpreted as being representative of the polar vortex. Recently, Plumb et al. (submitted manuscript, 1999) have suggested that a small amount of continuous mixing across the vortex edge throughout the winter could lead to distinct innervortex tracer relations that differ considerably from the extravortex relations or that compact relations might be lost inside the polar vortex. However, assuming the validity of assumption (1), the in situ observations of NO_y and N_2O obtained near 20 km during January and February 1989 suggest that the MkIV $\text{NO}_y/\text{N}_2\text{O}$ reference correlation was valid inside the vortex during the initial phase of denitrification in 1989 (Plate 2). We note that the remarkably good agreement between the MkIV and in situ observations of NO_y and N_2O supports the validity of both assumptions (1) and (2) because it would be highly unlikely that deviations from the assumptions would cancel in such a way to preserve the good agreement. However, it is not clear whether this agreement of innervortex and extravortex relations in January and February holds at higher altitudes and for all winters and whether it holds until mid-March, when diabatic descent inside the polar vortex commonly gets sufficiently slow [Rex et al., 1998; Knudsen et al., 1998; Rex et al., 1999] that any mixing occurring after this time would be well represented by our approach. The results of Michelsen et al. [1998] indicate that in mid-April 1993 the innervortex tracer relations deviated considerably from the extravortex relations, but it is not clear when this discrepancy developed. The question of whether and when distinct innervortex tracer relations develop needs to be addressed by tracer measurements within the vortex throughout the winter. We note that our analysis is valid only under the assumption that for the 1996-1997

winter the bulk of the mixing across the vortex edge took place after descent slowed down sufficiently (i.e., after approximately mid-March; estimations of diabatic descent rates based on observed temperatures and radiation transport calculations show that at 500 K the total descent after mid-March was of the order of only 10 K [Knudsen et al., 1998]). In section 4 we will further discuss the validity of this assumption for the 1996-1997 winter in the light of our results.

3.5. ER-2 Flight on April 26, 1997

3.5.1. Descent and mixing. Plate 4b shows the mixing ratio of N_2O calculated with the method described in section 3.3 for the innervortex end-members along the ER-2 flight track on April 26, 1997. The mixing ratios of the innervortex end-member were found to be between 25 and 40 ppbv. The associated approximate altitudes from which the innervortex end-members subsided through the winter are ~32-34 km (Plate 4c). The altitudes have been estimated using the mixing ratios of N_2O measured by the ER-2 and the MKIV extravortex profile of N_2O . An overall subsidence of ~13 km for air masses ending near 500 K (~20 km) is suggested by our analysis. This value agrees well with the overall descent of 13.8 km for air ending at 20 km that was derived by Abrams et al. [1996] for the Arctic winter 1992-1993 from ATMOS/ATLAS-2 data. Abrams et al. [1996] showed that this descent is consistent with the theoretical results of Manney et al. [1994] and Rosenfield et al. [1994]. The ratio between innervortex air and extravortex air in the sampled air masses has been calculated as described above and is shown in Plate 4d. For the observations discussed here, this ratio varies between 0.3 and 0.6 with higher fractions of innervortex air present at higher latitudes. As expected, high fractions of innervortex air correlate with high values of potential vorticity (Plate 4a).

3.5.2. Denitrification. Plate 4e compares observations of NO_y to $NO_{y,*}$ (NO_y based on the measured N_2O and the reference correlation between N_2O and NO_y) and $NO_{y,**}$ (NO_y calculated from the reference correlation, allowing for descent and isentropic mixing). Large differences between observed NO_y and $NO_{y,*}$ are apparent. In contrast, observations of NO_y agree well with $NO_{y,**}$ during most parts of the flight. This result suggests that most of the NO_y deficit found along the ER-2 flight track was caused by descent followed by isentropic mixing. However, during the northernmost part of the ER-2 flight on April 26, 1997, the mixing ratios of NO_y were smaller than $NO_{y,**}$, indicating that some denitrification had taken place.

This is further illustrated in Plate 5, where the observed NO_y/N_2O correlation, the $NO_{y,**}/N_2O$ correlation, and the extravortex reference correlation are shown. Measured NO_y agrees well with $NO_{y,**}$ for N_2O mixing ratios larger than 125 ppbv. For N_2O levels below 100 ppbv, a deficit of measured NO_y compared to $NO_{y,**}$ is visible. We interpret this 1-2 ppbv deficit in NO_y as the result of weak irreversible denitrification that occurred earlier in the winter. Since the denitrification probably occurred before the bulk of the mixing, it is reasonable to suggest that the deficit of NO_y originally caused by denitrification was diluted by subsequent mixing. Back projection of the NO_y deficit to pre-mixing conditions (dashed lines in Plate 5) shows that the original average degree of denitrification must have been approximately 2-3 ppbv (solid arrow in Plate 5) to cause the NO_y deficit observed in late April. Most likely the denitrification inside the polar vortex was characterized by patchy regimes of higher denitrified areas and areas without denitrification (as was observed on February 7, 1989; see Plate 2). In the weeks following the denitrification events, com-

paratively fast mixing inside the vortex probably led to an averaging of the degree of denitrification throughout the vortex yielding the 2-3 ppbv value reported above.

The weak denitrification reported here is consistent with the temperature structure of the 1996-1997 winter. PSC particles must grow to large sizes (of the order of 1-2 μm) to sediment with appreciable velocities [e.g., Salawitch et al., 1989]. Particle formation and growth models show that PSC particles reach sizes large enough to cause rapid denitrification once temperature falls below the frostpoint, due to efficient uptake of water [e.g., Drdla and Turco, 1991]. Differential growth may also lead to large particles for temperatures that are above the frostpoint but below the NAT (nitric acid trihydrate) equilibrium temperature (T_{NAT}) [Salawitch et al., 1989]. However, Santee et al. [1998] show that the phase change required to initiate differential growth most likely requires suppression of temperature below T_{NAT} continuously for a period of at least several days. In the Arctic the cold temperature region is normally displaced from the center of the vortex. As air masses circulate in the vortex, they alternately pass through cold ($T < T_{NAT}$) and warm regions every few days, so that severe denitrification in the Arctic may require the minimum temperature to drop below the frostpoint. Temperature analysis from the European Centre for Medium Range Weather Forecast shows that the synoptic temperatures dropped below the frostpoint (assuming 4.6 ppmv H_2O) only in limited areas (largest area $>2 \times 10^6 km^2 \approx 10\%$ of the vortex area) and only for two short periods, both only a couple of days long during mid and late February. The potential for formation of water ice PSCs during 1996-1997 was much smaller than in the winters of 1988-1989 and 1995-1996. Furthermore, in 1996-1997 the areas cold enough for synoptic water ice PSC formation were mainly at the 450 K level, which is below the air masses sampled by the ER-2 during its vortex flight. Considering some diabatic cooling during the late winter period, the air masses sampled by the ER-2 in late April at 500 K would have been even somewhat above 500 K during the cold periods in February. From vortex averaged radiative cooling rates calculated from the Universities' Global Atmospheric Modeling Programme (UGAMP), it was estimated that the subsidence between the coldest period and the April ER-2 flight was between 5-10 K potential temperature.

Our analyses have been based on ER-2 measurements of N_2O obtained by the ALIAS instrument. In situ measurements of the mixing ratio of N_2O are also obtained by the Airborne Tunable Laser Absorption Spectrometer (ATLAS) instrument for each ER-2 flight. There are slight differences between the ATLAS and ALIAS measurements of N_2O during limited segments of the two ER-2 flights considered here. However, we have repeated our entire analyses using the ATLAS measurements of N_2O , and we note that our overall conclusions are independent of which measurement of N_2O is used.

3.6. ER-2 Flight on June 30, 1997

During the ER-2 flight on June 30, 1997 remnants of the polar vortex were found at 510-530 K potential temperature, i.e., at slightly higher isentropic levels than during the flight of April 26. Plate 6 shows the CH_4/N_2O relation measured during this flight. The innervortex end-members that contributed to the air mass probed by the ER-2 had fairly constant N_2O mixing ratios of about 15-20 ppbv (Plate 7a). The associated initial altitude is ~37 km (Plate 7b), so that the overall descent for air masses ending at around 520 K in June is estimated to be ~16 km. Plate 7c shows that the fraction of innervortex air in the probed air masses varied between 20 and 70% for the air masses discussed here. The NO_y

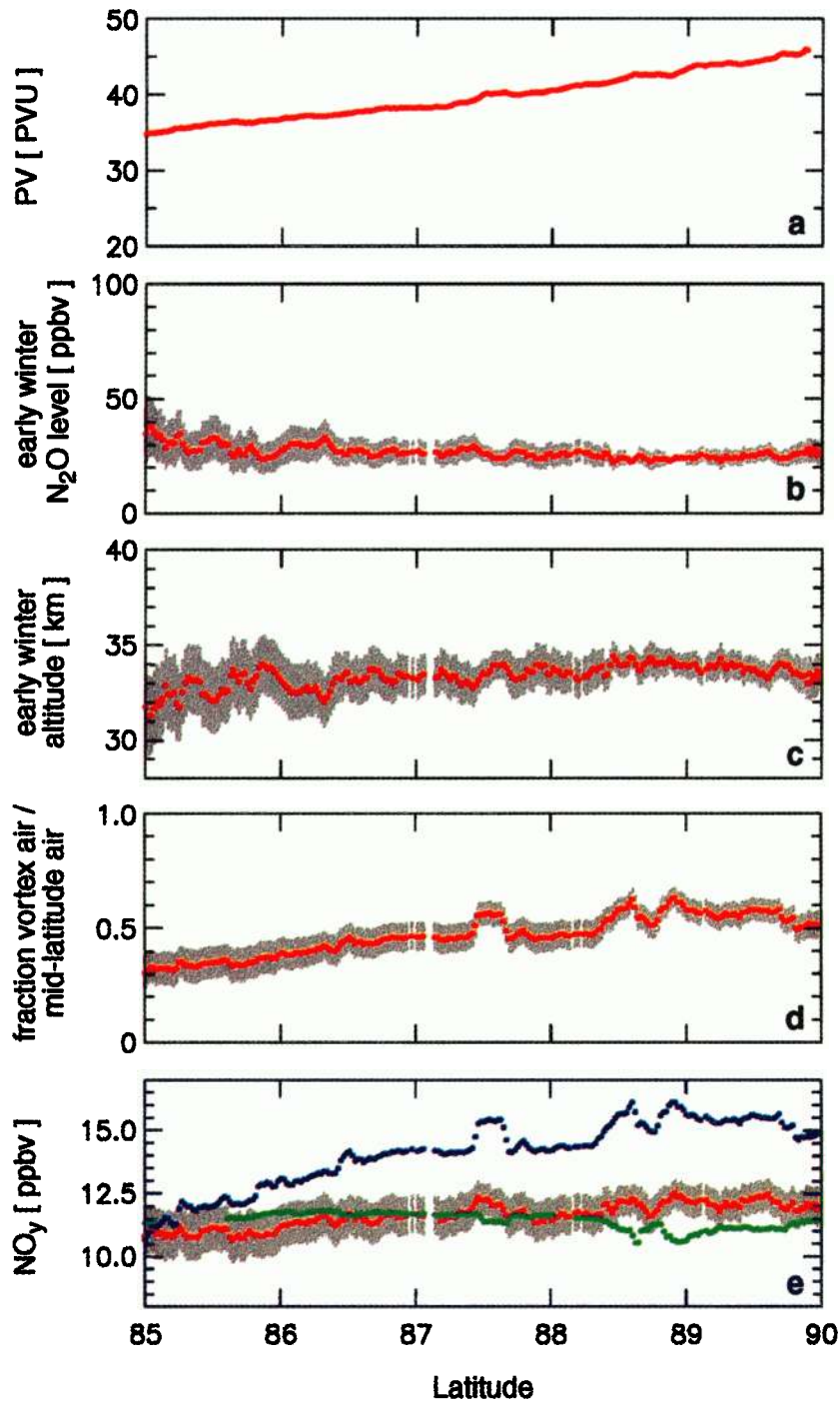


Plate 4. Measured and calculated quantities along the northbound track of the ER-2 flight on April 26, 1997. The gray shaded areas give an estimate of the uncertainty based on the errors in the measurements and the uncertainty in defining the properties of the extravortex mixing end-member. (a) Potential vorticity (1 Potential Vorticity Unit (PVU) = $10^{-6} \text{ K m}^2 \text{ s}^{-1} \text{ kg}^{-1}$), (b) calculated mixing ratio of N₂O for the innervortex mixing end-member, (c) corresponding approximate early winter altitude of the innervortex air, (d) fraction of innervortex air versus extravortex air in the mixed sample, (e) NO_y* which would have been predicted from the N₂O vmrs without considering mixing (blue), NO_y** predicted with consideration of mixing (red), and NO_y measured by the NOAA chemiluminescence instrument aboard the ER-2 (green).

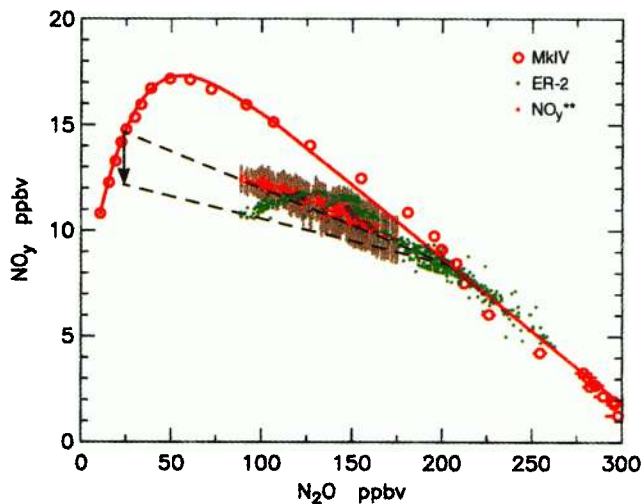


Plate 5. MkIV and ER-2 measurements as in Plate 1. The NO_y^{**} predicted for the air masses sampled by the ER-2 (red) and its uncertainty (gray, c.f. Plate 4) are compared with the measured NO_y (green). NO_y^{**} was calculated from the degree of descent and mixing derived from the $\text{CH}_4/\text{N}_2\text{O}$ correlation. The NO_y versus NO_y^{**} deficit at low N_2O levels is interpreted as a signature of irreversible denitrification. The premixing degree of denitrification in the air masses is estimated by a backprojection of the measured properties of the mixed sample to the properties of the innervortex mixing end-member (dashed lines). The estimated average premixing degree of denitrification in the sampled air masses is indicated by the arrow. Since the air masses inside the vortex are rapidly mixed and the denitrification typically occurs inhomogeneously, this degree of denitrification is likely the result of mixing of more heavily denitrified air masses with less or nondenitrified innervortex air.

observations agree very well with NO_y^{**} throughout the flight (Plate 8). This analysis reveals that the large deficits of NO_y compared with the extravortex reference can be explained entirely by descent and mixing. No indication for denitrification was found.

The vortex air masses sampled during the June 30, 1997, ER-2 flight were at higher potential temperature levels than those encountered during the April 26, 1997, flight. These air masses were well above the cold temperature region in February, and synoptic temperatures never dropped below the frostpoint in these air masses for the entire winter. Our finding that these air masses have not been significantly denitrified is consistent with the temperature structure of the 1996–1997 winter.

3.7. OMS Flight on June 30, 1997

On the same day as the latter ER-2 flight, the OMS balloon borne platform measured a profile of several trace species and encountered polar vortex remnants in two altitude regions around 500–520 K and 615–637 K potential temperature [Herman *et al.*, 1998]. The measured $\text{CH}_4/\text{N}_2\text{O}$ mixing ratios obtained during the balloon descent are plotted in Plate 9 together with the extravortex reference measured by the MkIV instrument. The ALIAS II observations are grouped into potential temperature ranges that are shown in different colors.

The mixing ratios of CH_4 and N_2O found in the vortex air masses around 495–520 K (blue points in Plate 9) lie along a mixing line very similar to that formed by the ER-2 observations obtained on the same day. The measurements of CH_4 and N_2O in air masses that have not been influenced by the polar vortex (black points in Plate 9) agree remarkably well with measurements made by the

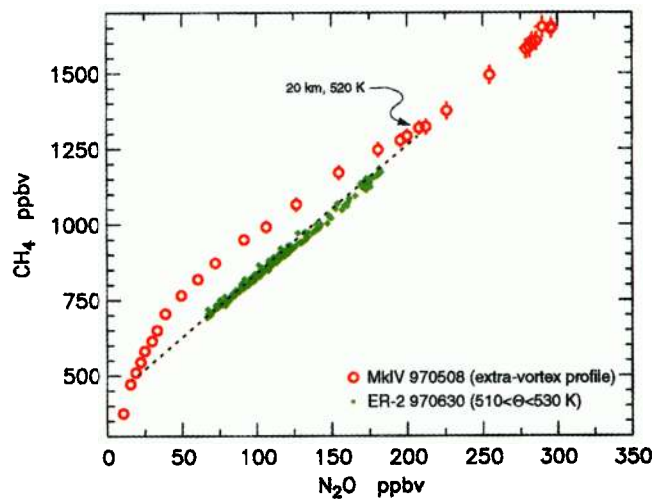


Plate 6. As Plate 3, but for the portion of the ER-2 flight at potential temperatures of 510–530 K near 65°N on June 30.

MkIV instrument on May 8, 1997 [see, also, Herman *et al.*, 1998]. These observations strongly support the assumption that the measurements from the different platforms may be compared directly without bias.

We now focus on the air masses probed between 615 and 637 K potential temperature (green in Plate 9). The $\text{CH}_4/\text{N}_2\text{O}$ relation of these air masses form a mixing line with a steeper slope than those indicated by the ER-2 and OMS measurements at lower altitudes. The mixing line meets the $\text{CH}_4/\text{N}_2\text{O}$ reference correlation at mixing ratios that correspond to the MkIV measurement obtained at 615 K potential temperature. This level coincides well with the potential temperature range probed by the OMS platform for the mixing line. The slope of the mixing line indicates that the innervortex end-member originated from well above the altitude region sampled by the MkIV instrument (dashed arrow in Plate 9). We used data from ATMOS/ATLAS-3 obtained during November of 1994 to identify the intersection of the extended mixing line with the reference correlation of $\text{CH}_4/\text{N}_2\text{O}$ (Plate 10). The intersection of the dashed line in Plate 10 with the extravortex reference indicates that the innervortex mixing member originated at an extremely low mixing ratio of N_2O and at a CH_4 mixing ratio of ~ 200 ppbv. Plate 11 shows that in autumn such low CH_4 levels are found between 40 and 60 km altitude, depending on latitude. Since the descending motion inside the vortex is coupled with a poleward motion at higher altitudes, it is not clear at which latitude and altitude the vortex air masses have been in autumn. According to Plate 11, it is possible that the vortex remnants at 615–637 K originated in the mesosphere.

The NO_y/CH_4 correlation measured by ATMOS/ATLAS-3 between 40 and 50°N (Plate 12, 50°N is the highest latitude sampled by the ATMOS instrument during the ATLAS-3 mission) has been used to calculate NO_y^{**} from the estimated CH_4 mixing ratios of the innervortex end-member for the air masses probed by the OMS platform between 615 and 637 K potential temperatures (Plate 13). At 60°N, the lifetime of NO_y is sufficiently long (during mid-October longer than 2 years below ~ 55 km; the lifetime has been estimated using the model described by Osterman *et al.* [1997] that probably no significant loss of NO_y during the descent occurred). However, the lifetime of N_2O at 50–55 km is only about 2 months (compare section 1) so that the quantitative results of this calculation might be slightly influenced by possible chemical changes of

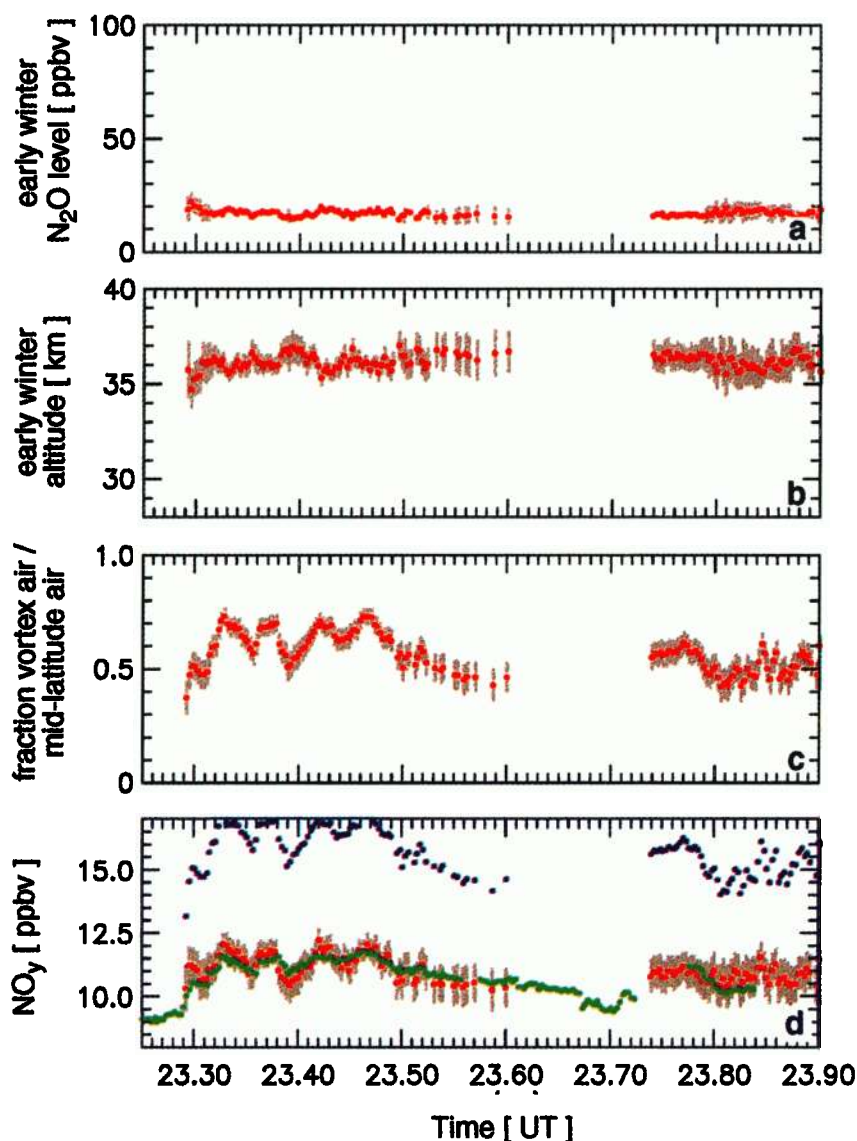


Plate 7. As Plate 4, but for the portion of the ER-2 flight at potential temperatures of 510–530 K near 65°N on June 30.

N_2O during the initial phase of the descent. Plate 13 shows that above 600 K, quite low $\text{NO}_y/\text{N}_2\text{O}$ ratios can be produced purely by mixing processes between subsided mesospheric air masses with extravortex air. This result supports the hypothesis of *Kondo et al.* [1999] that for altitudes above 20 km, very low values of NO_y can easily be mistaken for severe denitrification if dynamical processes are neglected.

4. “Continuous Mixing” Versus “Late Mixing”

Plumb et al. (submitted manuscript, 1999) presented a theoretical study of the evolution of tracer relationships inside the polar vortex in the presence of continuous weak mixing across the vortex edge. Their results show that if mixing across the vortex edge during the main phase of descent is strong enough to change the innervortex tracer relationships, then the approach used here would not be applicable in a quantitative manner. The critical aspect is the time at which mixing across the vortex edge first changes the tracer relations inside the polar vortex. If mixing changes the innervortex tracer relations during the main phase of the descent (approximate-

ly until early March), the results of Plumb et al. (submitted manuscript, 1999) demonstrate that transport properties inferred from one set of tracer relations should not be applied to a different set of tracer relations. If, however, the change in the tracer relations inside the vortex first occurs after descent has slowed sufficiently (i.e., after approximately mid-March), our approach is applicable, regardless of the precise nature of the isentropic mixing (i.e., whether it occurs as a single mixing event, a succession of a number of mixing events, or as continuous mixing after mid-March). We will refer to the latter scenario as “late mixing” and to the other scenario as “continuous mixing”. In the following we discuss data from two winters to address whether indications for continuous mixing can be identified in the real atmosphere.

4.1. Winter 1992–1993

The representation of ATMOS data from the ATLAS-2 mission (April 8–16, 1993) by *Michelsen et al.* [1998] suggests that over a broad range of potential temperatures, single, distinct, and near linear relations between NO_y and N_2O and between CH_4 and N_2O ex-

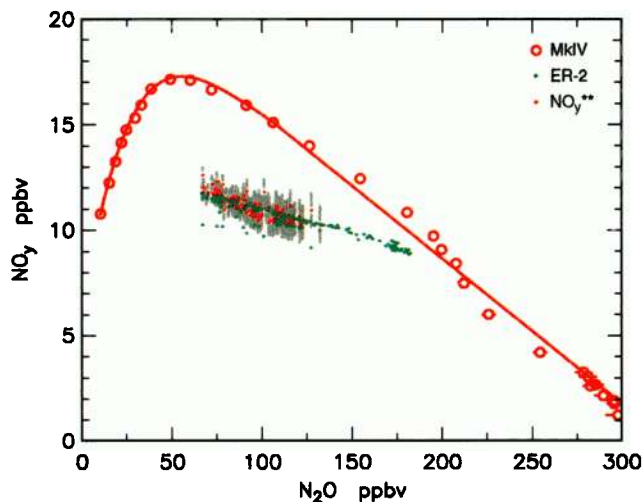


Plate 8. As in Plate 5, but for the ER-2 flight on June 30, 1997. The vortex remnants were encountered, while the ER-2 was between potential temperatures of 510 and 530 K; only ER-2 measurements between these levels have been plotted. No indication for denitrification is apparent.

isted inside the Arctic vortex during that winter. The existence of distinct compact innervortex tracer relations over a broad range of potential temperatures would suggest that continuous mixing had occurred (Plumb et al., submitted manuscript, 1999). However, in Michelsen et al. [1998] the large number of ATMOS measurements of individual NO_y species were averaged on a number of vertical levels, and the NO_y mixing ratio at each level was calculated to give an innervortex profile. This binning and averaging procedure may mask individual isentropic mixing lines. Isentropic mixing lines in tracer/tracer plots are formed by various individual measurements obtained on one potential temperature level. Statistically some of these individual measurements occur in air masses that contain a larger fraction of end-member A (e.g. innervortex air), others in air masses with larger fractions of end-member B (e.g. extravortex air). The statistical scatter of measurements at one isentropic level is needed to identify mixing lines in tracer/tracer plots.

If our approach of analyzing isentropic mixing lines is applied to the ATMOS/ATLAS-2 data, various distinct isentropic mixing lines in the $\text{NO}_y/\text{N}_2\text{O}$ relation are apparent. The isentropic analysis also reveals distinct mixing lines in the $\text{CH}_4/\text{N}_2\text{O}$ relation that are not apparent as given in Michelsen et al. [1998, Plate 2] because their analysis focusses solely on a few number of measurements obtained deep inside the Arctic vortex. The $\text{CH}_4/\text{N}_2\text{O}$ and $\text{NO}_y/\text{N}_2\text{O}$ mixing lines we identify have slopes that rise with increasing potential temperature and intersect with the extravortex relation in a manner similar to the mixing lines shown in Plate 9. This picture is compatible with the late mixing scenario but does not rule out continuous mixing either. A comprehensive analysis of the ATMOS data from 1992 to 1993 using the approach of isentropic mixing lines will be the subject of a future publication.

4.2. Winter 1996-1997

As mentioned in section 3.4, we currently cannot completely rule out the possibility that continuous mixing during descent inside the 1996-1997 vortex changed the innervortex tracer relations in a way that would hamper our approach. However, the good agreement between NO_y^{**} and the measured NO_y shown in Plate

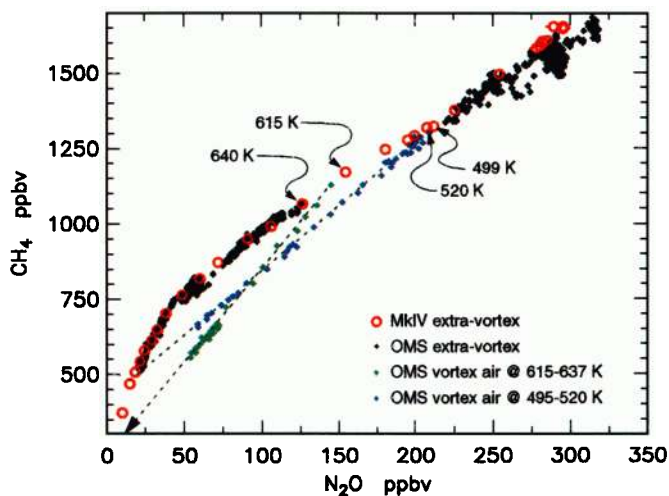


Plate 9. $\text{CH}_4/\text{N}_2\text{O}$ correlation observed by the ALIAS II instrument during the descent portion of the OMS balloon flight on June 30, 1997, compared to the MkIV measurements on May 8, 1997. The ALIAS II OMS data has been grouped into extravortex samples (black) and measurements obtained during the penetration of two distinct layers of vortex air remnants (green: 615-637 K, blue: 495-520 K). The observations within the vortex remnants reveal distinct mixing lines (dashed) for both potential temperature regions. The MkIV measurements on May 8, 1997, are given in red. The potential temperatures of the MkIV data points at the intersections with the OMS mixing lines are indicated.

8 indicates that this is probably not the case. Plumb et al. (submitted manuscript, 1999) demonstrated that if mixing during the main phase of descent had changed the innervortex tracer relations, the mixing lines observed in a $\text{NO}_y/\text{N}_2\text{O}$ plot and in a $\text{CH}_4/\text{N}_2\text{O}$ plot would intersect with the respective extravortex relations at differ-

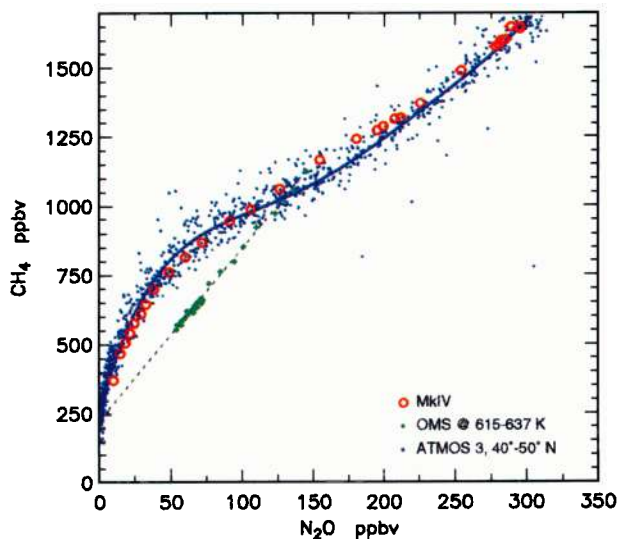


Plate 10. $\text{CH}_4/\text{N}_2\text{O}$ correlation for the OMS encounter of vortex remnants at 615 - 637 K potential temperature (green) compared with an extravortex reference correlation established by ATMOS/ATLAS-3 measurements obtained between 40° and 50°N in early November 1994 (blue dots, a fit to the data is plotted as blue line). The MkIV reference correlation from May 8, 1997, is shown in red.

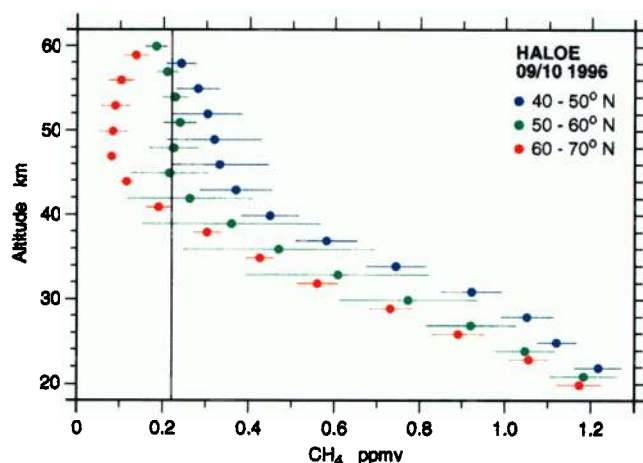


Plate 11. CH_4 profiles measured during September–October 1996 by the Halogen Occultation Experiment (HALOE)(data version 19) on the Upper Atmosphere Research Satellite between 40° and 70°N . The individual profiles were sorted into different latitude bands and were averaged into ± 1.5 km vertical bins. The error bars reflect the 1σ variability. The vertical line denotes the mixing ratio of CH_4 of the innervortex end-member for the OMS mixing line observed at 615–637 K potential temperature.

ent mixing ratios of N_2O . In contrast to that scenario, the success of our approach to precisely reproduce measured NO_y , as shown in Plate 8 demonstrates that the N_2O levels derived from both tracer plots agree very well. Given the temperature history of the air masses shown in Plate 8, it is unlikely that NO_y in these air masses was influenced by denitrification (compare section 3.6). It is highly unlikely that even if denitrification cannot be ruled out completely, the effect of denitrification would precisely cancel the effect of continuous early winter mixing to produce the good agreement between NO_y^{**} and measured NO_y shown in Plate 8.

Measurements of CH_4 and N_2O from two balloon flights at 68°N on February 11 and 22, 1997, show a near linear relationship [Kondo *et al.*, 1999], which indicates considerably mixing early in

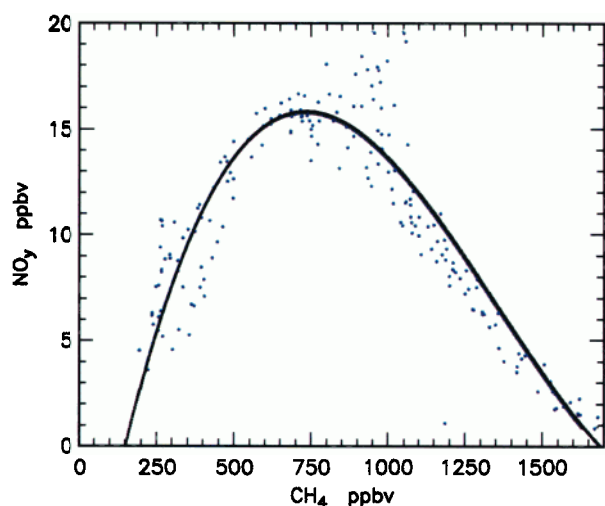


Plate 12. NO_y/CH_4 reference correlation measured by AT-MOS/ATLAS-3 between 40° and 50°N in early November 1994. The fit to the data has been used to estimate the mixing ratio of NO_y of the innervortex mixing end-member based on the estimated mixing ratio of CH_4 of that air mass (compare Plate 9).

the winter. However, these observations were obtained near the edge of the vortex and therefore may not be representative of conditions throughout the vortex.

We note that although our analysis indicates that any continuous mixing during the main phase of descent was probably not effective enough to influence the innervortex tracer relations in 1996–1997, this does not necessarily mean that such mixing could not influence the innervortex tracer relationships during other winters. The timing of mixing in a given winter is closely connected with the level of wave activity in the Northern Hemisphere during the respective winter. The temporal development of the wave activity throughout an Arctic winter varies tremendously from year to year, so that the tracer relationships inside the Arctic polar vortex may well be different from year to year. Plumb *et al.* (submitted manuscript, 1999) demonstrated the importance of detailed knowledge about the timing of any relevant mixing. The development of tracer/tracer relationships inside the Arctic polar vortex under a variety of meteorological conditions needs further research.

5. Conclusions

Mixing processes between subsided air masses from the polar vortex and midlatitude air can considerably alter otherwise well-established tracer correlations if their relationship is nonlinear. The combined measurements of NO_y , N_2O , and CH_4 obtained by the NOAA NO_y and the ALIAS instrument aboard the ER-2, the MkIV balloon-borne FTIR-spectrometer and the ALIAS II balloon borne tunable diode laser instrument during the POLARIS campaign provide detailed in situ tracer data in the mixed air masses as well as concurrently measured reference correlations for extravortex air.

A technique based on near linear isentropic mixing lines in the otherwise nonlinear correlation between CH_4 and N_2O has been used to quantify dynamically induced changes in the tracer relationships. The mixing lines at increasing potential temperature levels show an increasing slope and intersect with the reference correlation at their respective potential temperature. The informa-

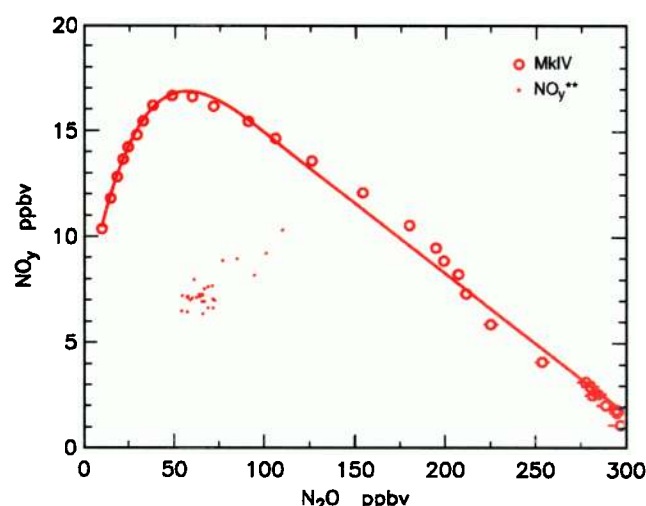


Plate 13. The $\text{NO}_y^{**}/\text{N}_2\text{O}$ correlation calculated for the air masses measured by OMS between 615 and 637 K on June 30 based on the degree of subsidence and mixing inferred from the CH_4 versus N_2O correlation. No denitrification has been assumed. MkIV data are the same as in Plate 1.

tion extracted from the CH₄/N₂O correlation has been used to calculate the abundance of NO_y** (the expected mixing ratio of NO_y accounting for descent and isentropic mixing) for the mixed air masses. The degree of denitrification has been derived by comparing observed NO_y with NO_y** . This approach is an extension of the approach of comparing NO_y with NO_y* [Fahey et al., 1990] to situations where the air masses have been subject to mixing across the vortex edge. Our analysis reveals evidence for only a small degree of denitrification in a limited region of the Arctic vortex sampled by the ER-2 flight on April 26, 1997, and no indication for denitrification for vortex air sampled at higher potential temperature levels during a flight on June 30, 1997. These findings are consistent with the synoptic-scale temperature history of the sampled air masses throughout the winter. The considerable deficit of NO_y compared with NO_y* (the mixing ratio of NO_y derived from the abundance of N₂O without considering mixing) during both flights, which would have been incorrectly interpreted as the result of denitrification in the 'traditional' approach, is actually mainly the result of descent and end-member mixing.

Our analysis supports the conclusions of Waugh et al. [1997], Kondo et al. [1999], and Michelsen et al. [1998] that it is important to use measurements of additional conserved species to accurately interpret changes in the NO_y/N₂O relation with respect to denitrification. The main uncertainty in our work lies in the definition of the innervortex tracer/tracer reference correlations that represent the composition of the innervortex end-members of the isentropic mixing process. We assume that tracer/tracer relations measured outside of the vortex also represent the composition of the inner-vortex end-members. Recent results from Plumb et al. (submitted manuscript, 1999) suggest that even weak continuous entrainment of extravortex air into the polar vortex during the main phase of descent could lead to innervortex tracer relationships that differ considerably from extravortex relations. We present data obtained inside the vortex near 20 km during POLARIS and a previous winter to support the validity of our assumptions concerning the inner-vortex tracer relations. However, it is not clear whether this result holds for other winters because wave activity that could lead to mixing across the vortex edge is quite variable from year to year. Measurements of tracer profiles inside the vortex during different phases of winter, as are planned for the upcoming NASA SAGE III Ozone Loss and Validation Expedition (SOLVE), will largely reduce the uncertainty of this type of analysis.

Acknowledgments. We thank P. Newman and L. Lait for providing the potential vorticity data used in Plate 4, James M. Russell III for providing the HALOE data used in Plate 11, and R. A. Plumb and D. W. Waugh for making their results available to us prior to publication. We also appreciate the efforts of the many personnel who contributed to the balloon launches and the ER-2 flights. Part of the research described in this paper was carried out by the Jet Propulsion Laboratory, California Institute of Technology, under a contract with the National Aeronautics and Space Administration.

References

- Abrams, M. C. et al., Trace gas transport in the Arctic vortex inferred from ATMOS ATLAS 2 observations during April 1993, *Geophys. Res. Lett.*, **23**, 2341-2344, 1996.
- Arnold F., V. Burger, K. Gollinger, M. Roncossek, J. Schneider, and S. Spreng, Observations of nitric acid perturbations in the winter Arctic stratosphere: Evidence for PSC sedimentation, *J. Atmos. Chem.*, **30**, 49-59, 1998.
- Brune, W. H., D. W. Toohey, J. G. Anderson, and K. R. Chan, In situ observations of ClO in the Arctic stratosphere: ER-2 aircraft results from 59°N to 80°N latitude, *Geophys. Res. Lett.*, **17**, 505-508, 1990.
- Brune, W. H., J. G. Anderson, D. W. Toohey, D. W. Fahey, S. R. Kawa, R. L. Jones, D. S. McKenna, and L. R. Poole, The potential for ozone depletion in the Arctic polar stratosphere, *Science*, **252**, 1260-1266, 1991.
- Chang, A. Y. et al., A comparison of measurements from ATMOS and instruments aboard the ER-2 aircraft: Tracers of atmospheric transport, *Geophys. Res. Lett.*, **23**, 2389-2392, 1996.
- Drdla, K., and R. P. Turco, Denitrification through PSC formation - a 1-D model incorporating temperature oscillations, *J. Atmos. Chem.*, **12**, 319-366, 1991.
- Fahey, D. W., K. K. Kelly, G. V. Ferry, L. R. Poole, J. C. Wilson, D. M. Murphy, M. Loewenstein, and K. R. Chan, In situ measurements of total reactive nitrogen, total water, and aerosol in a polar stratospheric cloud in the Antarctic, *J. Geophys. Res.*, **94**, 11299-11315, 1989.
- Fahey, D. W., K. K. Kelly, S. R. Kawa, A. F. Tuck, M. Loewenstein, K. R. Chan, and L. E. Heidt, Observations of denitrification and dehydration in the winter polar stratospheres, *Nature*, **344**, 321-324, 1990.
- Herman, R. L. et al., Tropical entrainment timescales inferred from stratospheric N₂O and CH₄ observations, *Geophys. Res. Lett.*, **25**, 2781-2784, 1998.
- Hintsa, E. J. et al., Dehydration and denitrification in the Arctic polar vortex during the 1995-1996 winter, *Geophys. Res. Lett.*, **25**, 501-504, 1998.
- Huebler, G., D. W. Fahey, K. K. Kelly, D. D. Montzka, M. A. Carroll, A. F. Tuck, L. E. Heidt, W. H. Pollock, G. L. Gregory, and J. F. Vedder, Redistribution of reactive odd nitrogen in the lower Arctic stratosphere, *Geophys. Res. Lett.*, **17**, 453-456, 1990.
- Kawa S. R., D. W. Fahey, L. E. Heidt, W. H. Pollock, S. Solomon, D. E. Anderson, M. Loewenstein, M. H. Proffitt, J. J. Margitan, and K. R. Chan, Photochemical partitioning of the reactive nitrogen and chlorine reservoirs in the high-latitude stratosphere, *J. Geophys. Res.*, **97**, 7905-7923, 1992.
- Keim, E. R. et al., Measurements of the NO_y-N₂O correlation in the lower stratosphere: Latitudinal and seasonal changes and model comparisons, *J. Geophys. Res.*, **102**, 13193-13212, 1997.
- Knudsen, B. M. et al., Ozone depletion in and below the Arctic Vortex for 1997, *Geophys. Res. Lett.*, **25**, 627-630, 1998.
- Kondo, Y. et al., NO_y-N₂O correlation inside the Arctic vortex in February 1997: Dynamical and chemical effects, *J. Geophys. Res.*, **104**, 8215-8224, 1999.
- Loewenstein, M. et al., New observations of the NO_y/N₂O correlation in the lower stratosphere, *Geophys. Res. Lett.*, **20**, 2531-2534, 1993.
- Manney, G. L., R. W. Zurek, A. O'Neill, and R. Swinbank, On the motion of air through the stratospheric polar vortex, *J. Atmos. Sci.*, **51**, 2973-2994, 1994.
- Michelsen, H. A., G. L. Manney, M. R. Gunson, and R. Zander, Correlations of stratospheric abundances of NO_y, O₃, N₂O, and CH₄ derived from ATMOS measurements, *J. Geophys. Res.*, **25**, 2777-2780, 1998.
- Nevison, C. D., and E. A. Holland, A reexamination of the impact of anthropogenically fixed nitrogen on atmospheric N₂O and the stratospheric O₃ layer, *J. Geophys. Res.*, **102**, 25519-25537, 1997.
- Notholt, J., P. von der Gathen, and S. Peil, Heterogeneous conversion of HCl and ClONO₂ during the Arctic winter 1992/1993 initiating ozone depletion, *J. Geophys. Res.*, **100**, 11269-11274, 1995.
- Oelhaf, H., G. et al., Correlative balloon measurements of the vertical distribution of N₂O, NO, NO₂, NO₃, HNO₃, N₂O₅, ClONO₂, and total reactive NO_y inside the polar vortex during SESAME, in *Polar Stratospheric Ozone*, edited by J. A. Pyle, et al., pp.175-178, Comm. of the Eur. Communities, Brussels, 1996.
- Osterman, G. B., R. J. Salawitch, B. Sen, G. C. Toon, R. A. Stachnik, H. M. Pickett, J. J. Margitan, J.-F. Blavier, and D. B. Peterson, Balloon-borne measurements of stratospheric radicals and their precursors: Implications for the production and loss of ozone, *Geophys. Res. Lett.*, **24**, 1107-1110, 1997.
- Plumb, R. A., and M. W. K. Ko, Interrelationships between mixing ratios of long-lived stratospheric constituents, *J. Geophys. Res.*, **97**, 10145-10156, 1992.
- Rex, M. et al., Prolonged stratospheric ozone loss in the 1995/96 Arctic winter, *Nature*, **389**, 835-838, 1997.
- Rex, M. et al., In-situ measurements of stratospheric ozone depletion rates in the Arctic winter 1991/92. A Lagrangian approach, *J. Geophys. Res.*, **103**, 5843-5853, 1998.
- Rex, M. et al., Chemical ozone loss in the Arctic winter 1994/95 as determined by the Match technique, *J. Atmos. Chem.*, **35**, 35-59, 1999.
- Rinsland, C. P., R. J. Salawitch, M. R. Gunson, S. Solomon, R. Zander, E. Mahieu, A. Goldman, M. J. Newchurch, F. W. Irion, and A. Y. Chang, Polar stratospheric descent of NO_y and CO and Arctic denitrification during winter 1992-93, *J. Geophys. Res.*, **104**, 1847-1861, 1999.
- Roche, A. E., J. B. Kummer, J. L. Mergenthaler, R. W. Nightingale, W. G.

- Uplinger, G. A. Ely, J. F. Potter, D. J. Wuebbels, P. S. Connel, and D. E. Kinnison, Observations of lower-stratospheric ClONO₂, HNO₃, and aerosol by the UARS CLAES experiment between January 1992 and April 1993, *J. Atmos. Sci.*, *51*, 2877-2902, 1994.
- Rosenfield, J. E., P. A. Newman, and M. R. Schoeberl, Computations of diabatic descent in the stratospheric polar vortex, *J. Geophys. Res.*, *99*, 16677-16689, 1994.
- Russell, J. M., III, C. B. Farmer, C. P. Rinsland, R. Zander, L. Froidvaux, G. C. Toon, B. Gao, J. Shaw, and M. Gunson, Measurements of odd nitrogen-compounds in the stratosphere by the ATMOS experiment on Spacelab-3, *J. Geophys. Res.*, *93*, 1718-1736, 1988.
- Salawitch, R. J., G. P. Gobbi, S. C. Wofsy, and M. B. McElroy, Denitrification in the Antarctic stratosphere, *Nature*, *339*, 525-527, 1989.
- Salawitch, R. J. et al., Loss of ozone in the Arctic vortex for the winter of 1989, *Geophys. Res. Lett.*, *17*, 561-564, 1990.
- Salawitch, R. J. et al., Chemical loss of ozone in the Arctic polar vortex in the winter of 1991-1992, *Science*, *261*, 1146-1149, 1993.
- Santee, M. L., W. G. Reed, J. W. Waters, L. Froidvaux, G. L. Manney, D. A. Flower, R. F. Jarnot, R. S. Harwood, and G. E. Peckham, Interhemispheric differences in polar stratospheric HNO₃, H₂O, ClO, and O₃, *Science*, *267*, 849-852, 1995.
- Santee, M. L., A. Tabazadeh, G. L. Manney, R. J. Salawitch, L. Froidvaux, W. G. Read, and J. W. Waters, UARS Microwave Limb Sounder HNO₃ observations: Implications for Antarctic polar stratospheric clouds, *J. Geophys. Res.*, *103*, 13285-13313, 1998.
- Sen, B., G. C. Toon, J. -F. Blavier, E. L. Fleming, and C. H. Jackman, Balloon-borne observations of midlatitude fluorine abundance, *J. Geophys. Res.*, *101*, 9045-9054, 1996.
- Sen, B., G. C. Toon, G. B. Osterman, J. -F. Blavier, J. J. Margitan, and R. J. Salawitch, Measurements of reactive nitrogen in the stratosphere, *J. Geophys. Res.*, *103*, 3571-3585, 1998.
- Toon G. C., The JPL MkIV interferometer, *Opt. and Photonic News*, *2*, 19-21, 1991.
- Toon G. C., C. B. Farmer, L. L. Lowes, P. W. Schaper, J. F. Blavier, and R. H. Norton, Infrared aircraft measurements of stratospheric composition over Antarctica during September 1987, *J. Geophys. Res.*, *94*, 16571-16596, 1989.
- Toon, G. C., C. B. Farmer, P. W. Schaper, L. L. Lowes, and R. H. Norton, Composition measurements of the 1989 Arctic winter stratosphere by airborne infrared solar absorption spectroscopy, *J. Geophys. Res.*, *97*, 7939-7961, 1992.
- Toon, G. C. et al., Comparison of MkIV balloon and ER-2 aircraft measurements of atmospheric trace gases, *J. Geophys. Res.*, this issue.
- Toon, O. B., P. Hamill, R. P. Turco, and J. Pinto, Condensation of HNO₃ and HCl in the winter polar stratospheres, *Geophys. Res. Lett.*, *13*, 1284-1287, 1986.
- Waibel, A. E., T. Peter, K. S. Carslaw, H. Oelhaf, G. Wetzell, P. J. Crutzen, U. Poschl, A. Tsias, E. Reimer, and H. Fischer, Arctic ozone loss due to denitrification, *Science*, *283*, 2064-2069, 1999.
- Waters, J. W., L. Froidevaux, W. G. Read, G. L. Manney, L. S. Elson, D. A. Flower, R. F. Jarnot, and R. S. Harwood, Stratospheric ClO and ozone from the Microwave Limb Sounder on the Upper Atmosphere Research Satellite, *Nature*, *362*, 597-602, 1993.
- Waugh, D. W. et al., Mixing of vortex air into middle latitudes as revealed by tracer-tracer scatterplots, *J. Geophys. Res.*, *102*, 13119-13134, 1997.
- Webster, C. R., R. D. May, D. W. Toohey, L. M. Avallone, J. G. Anderson, P. Newman, L. Lait, M. R. Schoeberl, J. W. Elkins, and K. R. Chan, Chlorine chemistry on polar stratospheric cloud particles in the Arctic winter, *Science*, *261*, 1130-1133, 1993.
- Webster, C. R., R. D. May, C. A. Trimble, R. G. Chave, and J. Kendall, Aircraft (ER-2) laser infrared absorption spectrometer (ALIAS) for in situ stratospheric measurements of HCl, N₂O, CH₄, NO₂ and HNO₃, *Appl Opt.*, *33*, 454-472, 1994.
-
- J. -F. Blavier, A. Y. Chang, M. R. Gunson, R. L. Herman, F. W. Irion, J. J. Margitan, R. D. May, E. J. Moyer, G. B. Osterman, M. Rex, R. J. Salawitch, D. C. Scott, B. Sen, G. C. Toon, C. R. Webster, Jet Propulsion Laboratory, California Institute of Technology, 4800 Oak Grove Drive, Pasadena, CA 91109-8009.
- T. P. Bui, Ames Research Center, National Aeronautics and Space Administration, Moffett Field, CA 94035.
- S. Donnelly, D. W. Fahey, R. S. Gao, E. Keim, J. Neuman, Aeronomy Laboratory, National Oceanic and Atmospheric Administration, Boulder, CO 80303.
- C. P. Rinsland, Langley Research Center, National Aeronautics and Space Administration, Mail Stop 401A, Hampton, VA 23681-2199.

(Received December 31, 1998; revised June 1, 1999; accepted June 23, 1999.)